Published in final edited form as:
Nat Neurosci. 2013 April ; 16(4): 407–415. doi:10.1038/nn.3333.

EGF transactivation of Trk receptors regulates the migration of newborn cortical neurons

Dirk Puehringer[1], **Nadiya Orel**[1], **Patrick Lüningschrör**[1], **Narayan Subramanian**[1], **Thomas Herrmann**[1], **Moses V Chao**[2], and **Michael Sendtner**[1]

[1]Institute for Clinical Neurobiology, University of Wuerzburg, Wuerzburg, Germany

[2]Molecular Neurobiology Program, Kimmel Center for Biology and Medicine, Skirball Institute of Biomolecular Medicine, New York University School of Medicine, New York, New York, USA

Abstract

The development of neuronal networks in the neocortex depends on control mechanisms for mitosis and migration that allow newborn neurons to find their accurate position. Multiple mitogens, neurotrophic factors, guidance molecules and their corresponding receptors are involved in this process, but the mechanisms by which these signals are integrated are only poorly understood. We found that TrkB and TrkC, the receptors for brain-derived neurotrophic factor (BDNF) and neurotrophin-3 (NT-3), are activated by epidermal growth factor receptor (EGFR) signaling rather than by BDNF or NT-3 in embryonic mouse cortical precursor cells. This transactivation event regulated migration of early neuronal cells to their final position in the developing cortex. Transactivation by EGF led to membrane translocation of TrkB, promoting its signaling responsiveness. Our results provide genetic evidence that TrkB and TrkC activation in early cortical neurons do not depend on BDNF and NT-3, but instead on transactivation by EGFR signaling.

During brain development, a complex pattern of neuronal connections is generated. This pattern is initially established by migration of newly generated neurons toward their final position in the cortical layers of the cerebral cortex. A pool of precursor cells in the ventricular zone and subventricular zone (SVZ) gives rise to most of the neurons and glial cells that form the brain in higher vertebrates[1–3]. These cells initially migrate toward the pial surface, known as the preplate. The preplate consists of two distinct cell types, the Cajal-Retzius cells, and a deeper zone of cells called the subplate cells. From this region, neuronal

Correspondence should be addressed to M.S. (sendtner_m@klinik.uni-wuerzburg.de).

Note: Supplementary information is available in the online version of the paper.

AUTHOR CONTRIBUTIONS

D.P. and M.S. designed the experiments. M.V.C. and T.H. provided tools and were involved in the early design of this study. D.P. performed most of the experiments. N.S. helped with the initial design and generation of lentiviruses for TrkB knockdown. T.H. generated viruses for dominant-negative Src. P.L. helped with biotin streptavidin cell surface protein isolation. N.O. helped with cell culture techniques for neural stem cells and performed the experiments. D.P. and M.S. wrote the manuscript.

COMPETING FINANCIAL INTERESTS

The authors declare no competing financial interests.

cell bodies migrate back to form the cortical plate where the cortical layers II–VI develop[4]. In rodents, neurogenesis starts early, around embryonic day 9 (E9), and most neurons that form the different layers in the mature cortex reach their positions by migrating radially toward the cortical plate such that those neurons that finally reside in the deeper layers of the cortex migrate first, and later arriving neurons give rise to the more superficial layers, thus generating an inside-out pattern[5–9].

Both intrinsic cues and growth factors influence mitosis, cell cycle exit, migration and synaptic differentiation of neurons in the developing cortex[10]. TrkB and TrkC, the receptors for BDNF and NT-3, are expressed early in developing neurons in the cortical ventricular zone and SVZ and during migration toward their final position in the cortex[11,12]. Inhibition of TrkB and TrkC via overexpression of dominant-negative constructs results in reduced numbers of proliferating neural precursor cells in the ventricular zone and SVZ, delayed migration and, ultimately, disturbed localization of neurons in the cortical layers[13]. Similar defects in migration of early cortical neurons were observed in mice in which the cytoplasmic tyrosines in the TrkB receptor that mediate docking of Src homology 2 domain-containing-transforming protein C (SHC) and fibroblast growth factor receptor substrate 2 (FRS2) adaptors and phospholipase Cγ (PLCγ) were inactivated, thereby abolishing activation of downstream signaling pathways once the tyrosine kinase activity of the TrkB receptors has been activated. However, it is unclear from these findings whether BDNF or NT-3, the ligands for TrkB and TrkC receptors, activate tyrosine kinases in early neurons to mediate these effects[13].

We examined the activation of TrkB and TrkC in the developing cortex of embryonic mice. We found that these receptors were activated at early stages of cortical development. Although TrkB and TrkC could be stimulated by BDNF and NT-3, the activation of these receptors was not affected in knockout mice lacking BDNF[14] and/or NT-3 (ref. 15). Unexpectedly, activation of EGFR by EGF in isolated cortical precursor cells resulted in a robust transactivation of TrkB and also TrkC. This transactivation is responsible for the effects of EGF on the migration of early cortical neurons from the VZ/SVZ toward the cortical layers. Our results suggest that the roles of TrkB and TrkC in newborn neurons of the developing cortex go beyond serving as specific receptors for BDNF and NT-3, and include the mediation and integration of additional signals, particularly those from the EGFR. Thus, TrkB and TrkC transactivation appears to be an essential mechanism for coordination of cortical differentiation when early neuronal cells migrate and integrate into the layers that form the cerebral cortex in higher vertebrates.

RESULTS

Ligand-independent activation of TrkB in cortical neurons

During development, high levels of TrkB are observed in the cerebral cortex long before BDNF expression reaches the high levels found in the adult brain. At E11, TrkB expression was detectable and its expression increased over the course of the next days to higher levels than those observed in early postnatal stages (postnatal day 4, P4; Fig. 1a). At E13, TrkB was highly expressed in cortical precursor cells of the SVZ and in doublecortin-positive neuronal cells of the early preplate (Fig. 1b). The SVZ cells, reflecting the neurogenic pool

of precursors that give rise to early neurons that migrate from the SVZ toward the preplate at the outer surface of the developing cerebral cortex, expressed activated TrkB, as determined by phosphorylation at the sites of SHC/FRS2 and PLCγ binding (Fig. 1b). These data are consistent with recent findings that TrkB and TrkC are involved in regulating mitosis[13] of neural precursor cells and migration of early neurons[13,16–18] in the developing cerebral cortex. In contrast with TrkB, endogenous BDNF levels are low during embryonic development and expression levels are only elevated after birth[11,19,20]. Thus, levels of TrkB activation, as determined using an antibody to the PLCγ binding site of this receptor, did not correlate with the availability of its ligand, BDNF. TrkB phosphorylation was higher at E13 than at P4 (Fig. 1a).

To investigate whether activation of TrkB occurs independently of neurotrophins at early stages of development, we determined the levels of TrkB phosphorylation in *Bdnf*$^{-/-}$ and *Ntf3*$^{-/-}$ mice[14,15]. No difference in TrkB activation was observed at E13 in the forebrains of *Bdnf*$^{-/-}$ mice (pTrk-PLCγ: 94.0 ± 9.4%, $n = 2$ embryos, $t = 0.6341$, degrees of freedom (df) = 1, $P = 0.6402$; pTrk-SHC: 96.6 ± 23.1%, $n = 2$ embryos, $t = 0.1459$, df = 1, $P = 0.9078$; phospho-tyrosine: 97.6 ± 8.6%, $n = 2$ embryos, $t = 0.2852$, df = 1, $P = 0.8231$; mean ± s.e.m., one sample *t* test) or *Ntf3*$^{-/-}$ mice (pTrk-PLCγ: 92.6 ± 9.2%, $n = 5$ embryos, $t = 0.8084$, df = 4, $P = 0.4642$; pTrk-SHC: 96.1 ± 9.7%, $n = 3$ embryos, $t = 0.4045$, df = 2, $P = 0.7250$; phospho-tyrosine: 110.4 ± 4.2%, $n = 2$ embryos, $t = 2.471$, df = 1, $P = 0.2448$; mean ± s.e.m., one sample *t* test) (Fig. 1c,d), as determined by TrkB immunoprecipitation and subsequent analysis with antibodies to the phospho-SHC and the phospho-PLCγ sites that recognized all members of the Trk receptor family, and phospho-tyrosine antibodies. In addition, *Bdnf*$^{-/-}$*; Ntf3*$^{-/-}$ double knockout mice did not show reduced activation of the TrkB isoform at 130 kDa (pTrk-PLCγ: 80.9 ± 10.6%, $n = 2$ embryos, $t = 1.807$, df = 1, $P = 0.3218$; pTrk-SHC: 76.3 ± 6.7%, $n = 2$ embryos, $t = 3.557$, df = 1, $P = 0.1745$; phospho-tyrosine: 95.4 ± 3.9%, $n = 2$ embryos, $t = 1.187$, df = 1, $P = 0.4458$; mean ± s.e.m., one sample *t* test; Fig. 1c,d), which was predominantly recognized by the TrkB antibody in these extracts and immunoprecipitates (Supplementary Fig. 1), indicating that neither BDNF nor NT-3 was necessary for the activation of this receptor at early stages of forebrain development.

EGF activates Trk receptors in cortical precursors

To determine the basis for these observations, we isolated neuronal cells from E12 forebrain[21]. These cell cultures consisted mainly of Pax6- and nestin-positive radial glia–like precursor cells, which formed neurospheres and could be differentiated by plating on laminin (Supplementary Fig. 2). These Pax6- and nestin-positive cultures also expressed relatively high levels of TrkB (Fig. 2a,b). The percentage of MAP2-positive neurons was low during the first 2 d after neurosphere-derived cells were plated on laminin (12.4 ± 3.2%, mean ± s.e.m.; Fig. 2c and Supplementary Fig. 2). However, most of these cells expressed nestin (Supplementary Fig. 2) and Pax6 (72.5 ± 5.1%, mean ± s.e.m.; Fig. 2c). Thus, they resembled freshly prepared cortical cells isolated from E11 forebrain (74.4 ± 4.6% Pax6^{+} and 9.2 ± 3.3% MAP2^{+}, mean ± s.e.m.; Fig. 2c). Phosphorylation of Trk receptors, as determined by a phospho-specific antibody to the PLCγ binding site of Trk receptors, was low, and only low levels of activation were observed when these cells were pulsed with

BDNF (Fig. 2a,b). Similarly, freshly prepared cells from E11 embryonic forebrain showed very little response to BDNF or NT-3, in contrast with cells isolated from later stages (E12 and E15), when the percentage of MAP2-positive fully differentiated neurons increased to levels higher than 75% (E12, 57.0 ± 5.1% $Pax6^+$ and 37.7 ± 3.4% $MAP2^+$; E15, 7.5 ± 3.0% $Pax6^+$ and 78.9 ± 3.5% $MAP2^+$; mean ± s.e.m.; Fig. 2c).

The relatively low response to BDNF or NT-3 in E11 primary cortical precursor cells and precursor cells derived from neurospheres from E12 forebrain prompted us to investigate the effects of other effectors that were previously identified as transactivators of TrkB[22–24]. Ligands for the glucocorticoid receptor (Supplementary Fig. 3a) did not induce increased TrkB activation, in contrast with EGF, which mediated high upregulation of TrkB phosphorylation in 5 min (EGF 5 min: 178.3 ± 12.1%, $n = 10$ independent experiments, $t = 6.460$, df = 9, $P = 0.0001$; EGF 120 min: 164.4 ± 15.5%, $n = 8$ independent experiments, $t = 4.145$, df = 7, $P = 0.0043$; EGF 360 min: 101.3 ± 4.6%, $n = 6$ independent experiments, $t = 0.2886$, df = 5, $P = 0.7845$; mean ± s.e.m., one sample t test; Fig. 2a,c). This response to EGF was not blocked by BDNF-neutralizing antibodies (Supplementary Fig. 3b) under conditions in which the effects of 10 ng ml^{-1} BDNF were blocked in primary neuronal cultures[23]. Treatment with EGF resulted in prolonged activation of the MAPK pathway, as shown by Erk1/2 phosphorylation (EGF 5 min: 195.8 ± 21.5%, $n = 5$ independent experiments, $t = 4.467$, df = 4, $P = 0.0111$; EGF 120 min: 196.7 ± 31.3%, $n = 4$ independent experiments, $t = 3.089$, df = 3, $P = 0.0538$; EGF 360 min: 130.0 ± 41.6%, $n = 3$ independent experiments, $t = 0.7222$, df = 2, $P = 0.5452$; mean ± s.e.m., one sample t test; Fig. 2a). The activation of TrkB could also be seen with antibodies that stained cultured cortical precursors. EGF treatment, in contrast with BDNF or NT-3, resulted in a massive upregulation of pTrk immunoreactivity in cultured nestin-positive cortical precursor cells in 5 min (pTrk-PLCγ: control, 15.6 ± 0.8; EGF, 93.7 ± 4.3; BDNF, 18.0 ± 0.9; NT-3, 21.2 ± 1.2 arbitrary units ± s.e.m.; $F = 274.1$, $R^2 = 0.9904$, $n = 3$; ≥55 cells per condition and experiment; Fig. 2b). Both the responsiveness to BDNF and to NT-3 in freshly prepared cultures from embryonic forebrain occurred later, at E12 (Fig. 2c), when the percentage of MAP2-positive neurons increased in cultures, indicating that early cortical precursor cells between E10 and E11 expressing nestin and Pax6 have stronger Trk phosphorylation in response to EGF than to BDNF or NT-3.

Src kinases mediate EGFR transactivation of Trk receptors

Previous data have shown that EGFR expression is high in Pax6- and nestin-positive precursor cells in the subventricular zone, and that expression is asymmetric in dividing precursor cells leaving the ventricular zone and SVZ when they start to migrate as early neurons to the cortical plate[25–27]. Consistent with these results, we found a high degree of TrkB and EGFR coexpression in neural cells in E13 forebrain (Fig. 2d).

Transactivation of TrkB by EGF in freshly prepared cortical precursor cells (Fig. 2c) and nestin-positive precursor cells derived from neurospheres (Supplementary Fig. 2) was not only observed with the antibody to the PLCγ site, but also with an antibody that recognizes the SHC/FRS2-binding domains (Fig. 3) in TrkB and other Trk receptors (pTrk-PLCγ: 5 min, 1,104.0 ± 234.2%, 15 min, 1,115.0 ± 258.4%, 45 min, 1,268.0 ± 317.9%, 90 min,

1,195.0 ± 238.7%, 180 min, 623.5 ± 52.6%, 300 min, 154.0 ± 19.7%; pTrk-Shc: 5 min, 374.6 ± 98.9%, 15 min, 318.0 ± 98.5%, 45 min, 328. 2 ± 108.6%, 90 min, 261.6 ± 102.4%, 180 min, 127.1 ± 11.0%, 300 min, 95.6 ± 7.1%; mean ± s.e.m.; Fig. 3a). In parallel, activation of Akt and Erk1/2 was observed over prolonged periods (pAkt: 5 min, 284.5 ± 17.4%, 15 min, 372.3 ± 17.3%, 45 min, 362.1 ± 17.4%, 90 min, 387.0 ± 28.7%, 180 min, 476.1 ± 39.4%, 300 min, 278.9 ± 15.1%; pErk1/2: 5 min, 1,116.0 ± 104.7%,15 min, 1,112.0 ± 84.1%, 45 min, 1,141.0 ± 84.2%, 90 min, 1,057.0 ± 81.5%, 180 min, 953.9 ± 88.9%, 300 min, 696.2 ± 53.9%; mean ± s.e.m.; Fig. 3a). To confirm the identity of the bands recognized by the pTrk antibodies, we transfected HA-tagged TrkB into the cultured cortical precursor cells and determined phosphorylation after immunoprecipitation with an antibody to HA. Only the band migrating at 130 kDa was recognized by the HA antibody in western blots of cell lysates (Fig. 3b). The activation of TrkB was also detected with the SHC site–specific antibody (Fig. 3a,b) and a phospho-tyrosine antibody (Fig. 3b).

Both the pTrk-SHC and the pTrk-PLCγ antibodies recognized a higher molecular weight band migrating at around 170 kDa. To determine whether this band represented TrkB, we performed shRNA-mediated lentiviral knockdown of TrkB, which led to reduced intensities of the bands for TrkB and pTrk-PLCγ at 130 and 170 kDa (Supplementary Fig. 4). A similar reduction was also observed with pTrk-SHC antibodies that were not specific for TrkB, but also recognized activated TrkA and TrkC (Supplementary Fig. 4). To exclude the possibility that this band represents activated EGFR, we performed pulldown experiments with an antibody to EGFR. No signal was detectable in the eluate using the pTrk-PLCγ antibody, in contrast with an antibody to the EGFR, which revealed a detectable band in the precipitate (Fig. 4a). The presence of phosphorylated EGFR was controlled by probing with a phospho-tyrosine antibody. Given that shRNA-mediated knockdown of TrkB did not fully abolish the bands representing the phosphorylated forms of TrkB at 170-and 130 kDa, we analyzed neural precursor cells from mice in which the TrkB protein is fully deleted[28]. Both the 130- and 170 kDa bands were still detectable with the pTrk-PLCγ antibodies (Supplementary Fig. 5a,b) and, in some experiments (Supplementary Fig. 4a), the intensity of the recognized bands was even higher. We then observed that both TrkC immunoreactivity and mRNA levels (Supplementary Fig. 5) were increased in TrkB knockout neural precursor cells (Supplementary Fig. 5a,c), indicating that TrkC is also recognized by the pTrk-PLCγ antibodies. Given that the cytosolic PLCγ sites are highly conserved in all members of the Trk family, this was not unexpected. To test this hypothesis, we designed lentiviral shRNA constructs for TrkC knockdown. At 72 h after viral infection, both the 130- and 170-kDa bands recognized by the pTrk-PLCγ antibodies were highly reduced, and, at 96 h after viral infection, they were virtually abolished by the expression of the shRNA construct used for TrkC knockdown (Supplementary Fig. 5a–c), indicating that the pTrk-PLCγ antibodies recognize TrkC, but not other tyrosine kinase receptors, including EGFR.

When the pTrk-SHC antibody that recognizes TrkB and TrkC was used for immunoprecipitation, the pTrk-PLCγ–immunoreactive bands were both precipitated after EGF stimulation (Fig. 4b). The observation that both the 130-kDa band and the 170-kDa bands reacted with independent TrkB antibodies, but not with EGFR antibodies, provides further evidence that the 170-kDa band includes TrkB and TrkC, which are transactivated after EGF addition.

The activation was abolished by inhibitors of Src kinases, PP1 (at 1 μM) and PP2 (at 100 nM), which have been found to be specific and sufficient to block transactivation of Trk receptors by G protein–coupled receptors in previous studies[29,30] (Fig. 3b). The involvement of Src family members was confirmed by using dominant-negative constructs for c-Src (dnSRC)[31] and Fyn (dnFYN)[32] in lentiviral gene transfer experiments (Fig. 3c,d). The expression of both constructs resulted in a significant reduction of pTrk-PLCγ immunoreactivity (GFP control, 100%; dnSRC, 63.3 ± 8.7%, $t = 4.199$, df = 2, $P = 0.0523$; dnFYN, 53.2 ± 12.8%, $t = 3.641$, df = 2, $P = 0.0679$; dnSRC and dnFYN, 48.1 ± 7.7%, $t = 6.761$, df = 2, $P = 0.0212$; PP1 and PP2, 10.6 ± 4.2%, $t = 21.36$, df = 2, $P = 0.0022$; $n = 3$ independent experiments, one sample *t* test,) that correlated with the transduction efficacy of the lentiviruses at about 40%, suggesting that c-Src and Fyn are necessary for transactivation of TrkB after EGF treatment. Furthermore, an inhibitor for EGFR signaling[33] completely abolished the activation of TrkB in the cultured cortical precursor cells (Fig. 3b). Together with the data from the Src inhibitor experiments, these results indicate that c-Src and Fyn are necessary for transactivation of TrkB and TrkC after EGF treatment.

EGFR transactivation elevates cell surface levels of TrkB

To study the cellular basis of why EGF signaling is more potent than BDNF or NT-3 at activating TrkB and TrkC in early E11 cortical precursor cells or in neurosphere-derived cortical precursor cells, we first investigated the subcellular localization of TrkB before and after EGF treatment. TrkB staining in untreated cultured cortical precursor cells was confined to intracellular compartments (Figs. 4 and 5). This suggests that TrkB, and possibly TrkC, are retained in the endoplasmic reticulum and Golgi compartment in these early cortical precursor cells. To find the cause for this retention, we studied the effect of various deglycosylating enzymes and found that an incubation with peptide N-glycosidase F (PNGase F) shifted the size of the higher molecular weight band for TrkB to 145 kDa (Fig. 4c). Other glycosidases, including β-1,4-galactosidase and β-N-acetylglucosaminidase, which cleave processed glycosyl side chains typically found in cell surface–exposed proteins[34], did not shift the molecular weight. To test whether the high degree of N-glycosylation of TrkB found in early cortical precursor cells influences its subcellular distribution, we treated these cells for 12 h with tunicamycin. This treatment, which blocks the first step of N-glycosylation in the endoplasmic reticulum, resulted in enhanced membrane translocation of TrkB (Fig. 4d) in these cells and a shift of the 170-kDa form of TrkB to about 130 kDa (Fig. 4e). When TrkB was able to translocate to the cell membrane under these conditions, BDNF phosphorylated the 130-kDa form that resulted from reduced glycosylation (Fig. 4e), indicating that this band reflects TrkB. A high degree of N-glycosylation, as found in the 170-kDa form of TrkB in E11 primary cortical precursors or neurosphere-derived precursors, has also been found to be involved in sorting of other proteins, such as occludin, to the apical pole of the cell membrane[35], and increased N-glycosylation of the beta1 subunit of the Na-K-ATPase results in an increased fraction of this protein being distributed to the apical membrane of polarized epithelial cells[36]. Thus, we investigated whether activation of N-hyperglycosylated TrkB via EGFR signaling affects the trafficking of TrkB to the cell membrane.

Within 30 s of EGF treatment, TrkB and pTrk immunoreactivity became detectable at the cell surface (Fig. 5a). To confirm this finding, we performed stimulated emission depletion (STED) microscopy (Fig. 5b). In untreated cortical precursor cells, STED microscopy only revealed small vesicle-like structures. Following EGF treatment, signals for TrkB and pTrk rapidly moved from intracellular compartments to the cell surface (Fig. 5b). In addition, avidin pulldown experiments were performed with cells in which cell surface proteins were biotinylated. Again, EGF treatment led to a rapid increase of cell surface–exposed TrkB (178.3 ± 20.4%, $t = 6.657$, df = 2, $P = 0.0218$, $n = 3$ independent experiments, one sample t test; Fig. 5c), which was blocked by the EGFR inhibitor PD153035 (120.5 ± 19.2%, $t = 1.854$, df = 2, $P = 0.2049$, $n = 3$ independent experiments, one sample t test; Fig. 5c).

This effect was physiologically relevant, as the translocation was not observed in cortical precursor cells isolated from *Egfr*$^{-/-}$ mice[37] (Supplementary Fig. 6a). When cells were fixed immediately, 2 s after EGF exposure, activation of intracellular TrkB was observed using the pTrk-PLCγ antibody (Supplementary Fig. 6b). At 10 s after EGF exposure, TrkB translocation to the cell membrane was observed (Supplementary Fig. 6b), indicating that transactivation of TrkB in intracellular compartments occurs prior to translocation to the cell surface. Similarly, confocal analysis of brain sections from E13 embryos revealed that most cells in the ventricular zone and SVZ expressed TrkB at intracellular sites resembling vesicular and intracellular locations, whereas cells that had already reached the cortical plate exhibited TrkB as a relatively continuous staining on the cell surface (Fig. 5d). Taken together, these data indicate that TrkB activation in developing cortical neurons leads to translocation of this receptor from an intracellular endoplasmic reticulum–like compartment to the cell surface and that EGFR signaling is more important than endogenous BDNF or NT-3 for TrkB and TrkC activation in the early neurons that start to migrate out of the ventricular zone and SVZ.

Migration of cortical neurons is disturbed in *Egfr*$^{-/-}$ mice

To confirm this hypothesis, we investigated *in vivo* TrkB/TrkC phosphorylation in the forebrain of E13 *Egfr*$^{-/-}$ mouse embryos (Fig. 6a). Quantitative analysis of densitometric immunoblot scans revealed that pTrk levels were significantly reduced in *Egfr*$^{-/-}$ mouse brain (pTrk-PLCγ, 89.1 ± 5.2% reduction, $t = 16.99$, df = 2, $P = 0.0034$; pTrk-SHC, 96.3 ± 1.8% reduction, $t = 53.62$, df = 2, $P = 0.0003$; phospho-tyrosine, 96.2 ± 1.9% reduction, $t = 49.64$, df = 2, $P = 0.0004$; mean ± s.e.m., $n = 3$ embryos, one sample t test), whereas TrkB protein levels were not altered (Fig. 6b). Taken together with the observation that lack of endogenous BDNF, NT-3 or both factors did not alter TrkB phosphorylation at this developmental stage (Fig. 1c,d), these data indicate that transactivation of TrkB via EGFR signaling is the major activator of TrkB in the developing cortex at this stage.

Recent studies have provided evidence that TrkB and TrkC activation influence migration of early neurons from the ventricular zone and SVZ to the developing cortical plate[13,16]. In *Egfr*$^{-/-}$ mice, the layer of neurons in the cortical plate corresponding to layers V and VI of the postnatal brain, which comprises large, pyramidal cell-like neurons, was thinner at E16 (Fig. 6c), and the number of TrkB- positive cells in this layer was significantly reduced (*Egfr*$^{+/+}$, 51.3 ± 4.5%; *Egfr*$^{-/-}$, 45.5 ± 3.0%; $t = 4.570$, df = 34, $P < 0.0001$, mean ± s.e.m.,

unpaired *t* test, counts from six sections from each of three embryos per genotype). Furthermore, the number of TrkB-positive neurons in layer I was increased ($Egfr^{+/+}$, 47.9 ± 1.0%; $Egfr^{-/-}$, 53.2 ± 0.7%; $t = 4.233$, df = 34, $P < 0.0002$, mean ± s.e.m., unpaired *t* test, counts from six sections from each of three embryos per genotype), as was the number of TrkB-positive cells in the ventricular zone and SVZ and the intermediate zone ($Egfr^{+/+}$, 0.4 ± 0.1%; $Egfr^{-/-}$, 0.8 ± 0.1%; $t = 4.465$, df = 34, $P < 0.0001$, mean ± s.e.m., unpaired *t* test, counts from six sections from each of three embryos per genotype), where migrating neurons are expected. Co-staining of TrkB with MAP2 revealed that these TrkB-positive migrating cells in the intermediate zone were indeed neurons (Fig. 6d).

Similar findings were made after BrdU injection at E13 3 d later in E16 wild-type and $Egfr^{-/-}$ mice (Supplementary Fig. 7). The number of BrdU cells that had reached layer V/IV at E16 was significantly ($P < 0.005$) reduced in $Egfr^{-/-}$ brain and was correspondingly increased ($P < 0.005$) in the cortical plate and marginal zones (Supplementary Fig. 7b). We found no differences in the total numbers of BrdU- positive cells in $Egfr^{-/-}$ and $Egfr^{+/+}$ mice (Supplementary Fig. 7c). This is consistent with the observations made with mice in which the SHC/FRS2 and PLCγ sites of TrkB were inactivated[16]. In these mutant mice, migration of early neurons from the ventricular zone and SVZ to the cortical plate is delayed. To investigate whether TrkB transactivation by EGF stimulates migration of early neurons, we plated these cells on laminin-coated cover slips with stripes of EGF or bovine serum albumin (BSA), adopting a technical setup that was used previously to study axon path finding and neural migration[38,39]. At 6 h after plating, early cortical neurons were equally distributed on BSA and EGF. At 20 h, most of the cells were found on stripes coated with EGF (layer I: EGF, 66.6 ± 2.3%; BSA, 33.4 ± 2.3%; $P < 0.001$; layer II: EGF, 59.8 ± 1.7%; BSA, 40.1 ± 1.7%; $P < 0.001$, $F = 13.29$, $R^2 = 0.2598$, mean ± s.e.m., one-way ANOVA; Fig. 6e). No enhanced cell death of cortical precursor cells was observed in regions coated with BSA (data not shown). Cultures where all stripes were coated with BSA or EGF were also analyzed. In such cultures, the distribution of cells stayed the same, no migration was observed (layer III: BSA, 49.2 ± 1.9%; BSA, 50.8 ± 1.9%; $P > 0.05$; layer IV: EGF, 49.1 ± 1.8%; EGF, 50.8 ± 1.8%; $P > 0.05$, $F = 13.29$, $R^2 = 0.2598$, mean ± s.e.m., one-way ANOVA). Cells stained with antibodies to pTrk-PLCγ showed an asymmetrical staining with an accumulation of activated TrkB at the migration front toward the source of EGF (Fig. 6f and Supplementary Fig. 8). When BDNF stripes were used, early cortical neurons migrated only with low efficacy toward BDNF. In contrast, when EGF was added to the medium, the percentage of cells that migrated toward the BDNF coated stripes significantly increased (without EGF, 55.6 ± 2.3%; with EGF, 68.5 ± 2.1%; $P < 0.001$, $F = 49.20$, $R^2 = 0.5027$, mean ± s.e.m., one-way ANOVA), whereas the proportion of cells on non-BDNF stripes decreased (without EGF, 44.5 ± 2.3%; with EGF, 31.6 ± 2.1%; $P < 0.001$, $F = 49.20$, $R^2 = 0.5027$, mean ± s.e.m., one-way ANOVA), indicating that EGF enhances the capacity of early cortical neurons to migrate toward BDNF coated substrates (Fig. 6g).

We did not observe alterations in the mitosis of early TrkB-positive cells in the ventricular zone and SVZ (Supplementary Fig. 7) in $Egfr^{-/-}$ embryonic forebrain, as was observed after injection of constructs encoding dominant-negative forms of TrkB or shRNA for suppression of TrkB[13] into ventricular zone and SVZ precursor cells. However, EGFR was

only expressed in cells that migrated out of the SVZ, and a small population of TrkB-positive cells existed in the ventricular zone and SVZ that were strongly stained for TrkB, but not for EGFR (Fig. 2d), suggesting that mechanisms other than transactivation by EGFR signaling could lead to a mitotic effect via TrkB in this population of EGFR-negative cortical precursor cells. We also did not observe increased apoptosis of TrkB-positive cells at E13 (Supplementary Fig. 9) in *Egfr*$^{-/-}$ mouse embryos, indicating that TrkB activation was not necessary for the survival of early cortical neurons during migration and the early stages at which the different cortical layers form.

DISCUSSION

Extracellular factors are important for neural differentiation. Some of these, such as sonic hedgehog and FGF2, act as morphogens: they are distributed in a gradient and evoke different cellular responses, depending on concentration. Neurotrophins and ligands for the EGFR are involved in guiding migration of newly generated neurons in the developing cortex[25], and there is evidence for chemotactic responses of axonal growth cones to locally applied BDNF that are mediated via the TrkB receptor[40–42]. Whether these guidance mechanisms also act on migrating early neurons in the cortex, and whether BDNF is responsible for guiding neurons from the ventricular zone and SVZ to the cortical plate, is less established. We found that TrkB activation was not reduced in BDNF- or NT-3–deficient brain, indicating that the activation of TrkB receptors in early neuronal cells that migrate from the ventricular zone and SVZ toward the cortical plate is ligand independent. In contrast, TrkB activation was reduced in the developing forebrain of *Egfr*$^{-/-}$ mice in which the migration of neuronal cells from the ventricular zone and SVZ to the cortical plate is disturbed, and suppression or inhibition of c-Src or Fyn, which are known to mediate transactivation of TrkB[29,30,43] at intracellular compartments, abolished this transactivation.

Transactivation led to asymmetric recruitment of TrkB to the cell membrane and accumulation of the receptor toward the migrating front of these cells. In the developing forebrain, EGFR expression peaks around E13, the time when neurogenesis is at its maximum. Both in the ventricular zone and the SVZ in mouse embryos, EGFR has been found to be asymmetrically distributed in a subpopulation of about 20% of the dividing cortical precursor cells[27], indicating that EGFR could be involved in controlling the rate of mitosis and migration in developmental corticogenesis. Together with our data, these observations suggest that the asymmetric location of the EGFR in early migrating neurons that exit the ventricular zone and SVZ determines the asymmetric translocation of TrkB and TrkC into the cell membrane of these early migrating neuronal cells. Indeed, as we found, and as shown previously[44], defective migration and disturbed formation of cortical layers is a predominant phenotype in EGFR-deficient mice. Similar observations have been made in mice in which TrkB activity was repressed by overexpression of dominant-negative constructs[13] and in mice in which the binding sites for molecules leading to downstream responses after receptor activation are inactivated[16].

It is not clear whether EGFR and TrkB/TrkC also act together in stimulating mitosis of dividing neural precursor cells in the ventricular zone and SVZ[13,45]. Experiments in which dominant-negative TrkB or TrkC constructs are overexpressed in these cells have shown

that apoptosis is enhanced and mitosis is reduced in neural precursor cells of the ventricular zone and SVZ[13]. Endogenous TrkB is mainly located at intracellular compartments in these cells, both *in vivo* and *in vitro* in freshly isolated forebrain neural precursor cells and neurosphere-derived cells. We did not observe enhanced cell death in the brain of EGFR-deficient developing forebrain. On the other side, robust activation of TrkB was observed in TrkB-positive cells in the ventricular zone and SVZ between E11 and E13, and the levels of TrkB activation were not reduced in BDNF- or NT-3–deficient mouse brain at these developmental stages, indicating that EGFR activation might not be the only mechanism that leads to transactivation of TrkB and TrkC in these early neurons.

In the adult nervous system, activation of EGFR, either by EGF or TGFα[46], induces mitosis of transit-amplifying type C neural precursor cells in the ventricular zone and SVZ. Moreover, EGF signaling leads to the arrest of neuroblast production and rapid migration of SVZ cells to various positions of the cerebral cortex. Most ligands for the EGFR are bound to membranes and to the extracellular matrix in the developing cortex, and this could lead to asymmetric membrane translocation of TrkB at the migrating front of cortical precursor cells. This explanation is also consistent with the observation that EGFR and TrkB activation cooperate in ovarian cancer cells and stimulate migration of these tumor cells[47]. The translocation of TrkB to the cell surface toward the source of EGF therefore reflects an important step in the differentiation of cortical neurons that occurs during migration toward the cortical plate. Cortical neurons could become responsive to neurotrophins once they reach their final position in the developing cortex and when synaptogenesis starts. Elevated neural activity, as shown previously by treatment of CNS neurons with cAMP or depolarization, could then contribute to the elevation of TrkB cell surface expression and the development of responsiveness to BDNF[48]. This interpretation is supported by our finding that responsiveness to BDNF developed later than TrkB transactivation via EGFR in primary cultures of forebrain neurons, in parallel with the occurrence of MAP2-positive neurons in such cultures (Fig. 2c).

The paradox of high levels of TrkB activation at early stages, when nestin- and Pax6-positive precursor cells are predominant, and the relative absence of BDNF can be explained by transactivation by other growth factor signals. As BDNF expression is only elevated after birth, when most synapses in the developing cortex are formed, these findings indicate that the TrkB receptor could act as an integrative coordinator of distinct signaling pathways that modulate neural differentiation. Recent findings from mouse models in which TrkB is specifically deleted in hippocampal precursor cells in the adult support this model. These mice have defects in neural migration into the granule cell layer[49] and defects in dendritic development[50], and they lack responsiveness to antidepressant therapies and have corresponding behavioral abnormalities. Whether this is a result of the shutdown of responses to BDNF or of additional transactivating effects from EGFR and other receptors will be an interesting topic for future studies.

ONLINE METHODS

Mice

Egfr$^{+/-}$ mice[37] on a mixed C57Bl/6 × MF1 background were crossed to produce homozygous mutant (*Egfr*$^{-/-}$) mice. *Bdnf*$^{+/-}$ (ref. 14) and *Ntf3*$^{+/-}$ (ref. 15) mice were intercrossed to produce homozygous *Bdnf*$^{-/-}$ and *Ntf3*$^{-/-}$ offspring. Double heterozygous *Bdnf*$^{+/-}$*; Ntf3*$^{+/-}$ mice were intercrossed to produce *Bdnf*$^{-/-}$*; Ntf3*$^{-/-}$mutant mice. *Ntrk2*$^{+/-}$ mice[28] were obtained from University of California, Davis (MMRRC:000188, B6;129S4-*Ntrk2*<*tm1Rohr*>) and maintained on a C57Bl/6 background. All mouse procedures were approved by the local authorities of the Regierung von Unterfranken.

Antibodies and reagents

Antibodies to TrkB (Santa Cruz, H-181, 1:500), TrkB (Millipore, #07-225, 1:1,000; BD Bioscience, #610101, 1:500), phospho–Trk-PLCγ (lot 18664, 1:2,000)[51], phospho–Trk-SHC (pTrkA^{Y490}, Cell Signaling, #9141, 1:1,000), TrkC (Cell Signaling, C44H5, 1:1,000), phospho-Akt (Ser473, Cell Signaling, #9271, 1:1,000), Akt (Cell Signaling, #9272, 1:1,000), Erk1 and Erk2 (Santa Cruz, K23, 1:1,000), phospho-Erk1/2 (Thr202/Tyr204, Cell Signaling, #9106, 1:1,000), GFP (Santa Cruz, #sc-8334, 1:2,000), EGFR (Santa Cruz, #sc-03, #sc-81449, 1:1,000; R&D Systems, #AF1280, 1:200), MAP2 (Millipore, AB5622, 1:1,000), Doublecortin (DcX, Millipore, #AB2253, 1:6,000), Nestin (Millipore, rat-401, 1:200), GAPDH (Millipore, 6C5, 1:4,000), Tuj1 (Neuromics, #MO15013, 1:1,000; Hybridoma supernatant from E7, Developmental Studies Hybridoma Bank, 1:100), Pax6 (Hybridoma supernatant, Developmental Studies Hybridoma Bank, 1:50), HA-epitope (Covance, 16B12, 1:1,000), phospho-tyrosine (Santa Cruz, PY99, 1:1,000), and panCadherin (Abcam, CH-19, 1:1,000) were used. Fluorescence and peroxidase-conjugated secondary antibodies were from Jackson ImmunoResearch Laboratories. Src family kinase inhibitors PP1, PP2 and EGFR inhibitor PD153035 were purchased from Calbiochem, protease inhibitor from Roche Diagnostics, phosphatase inhibitor and tunicamycin from Sigma, and EGF and basic FGF from Cell Concepts.

Cortical precursor cell culture

Cortical precursor cells were isolated as previously described[21] and cultured with bFGF and EGF at 20 ng ml^{-1} each. Lipofectamine 2000 (Invitrogen) was used for transfection. When cells reached 70–80% confluence, bFGF and EGF were withdrawn and cells were cultured for additional 24 h. Factor treatment was performed for indicated durations; pre-treatment with pharmacological inhibitors was performed for 1 h or as indicated for the individual experiments.

Protein isolation, immunoprecipitation and western blotting

Plated cortical precursors were harvested, washed twice with ice-cold phosphate-buffered saline (PBS) and directly lysed in immunoprecipitation buffer (25 mM Tris-HCl pH 7.5, 150 mM NaCl, 2 mM EDTA, 2 mM EGTA, 10% glycerol (vol/vol), 0.1% NP-40 (vol/vol), 2 mM NaVO, 50 mM NaF) with protease and phosphatase inhibitors. Dissected forebrains were frozen in liquid nitrogen, homogenized in immunoprecipitation buffer and centrifuged

at 20,800*g* for 20 min at 4 °C. The protein content of clarified supernatants was assessed using the Bio-Rad protein assay. We used 200 μg of total protein for immunoprecipitation of overexpressed HA-TrkB in cortical precursor cells and 250 μg total protein for immunoprecipitation of endogenous TrkB from brain tissues. Protein lysates were precleared with Protein-G–Agarose (Roche) for 1 h at 4 °C. Protein pulldown was performed using 1–4 μg primary antibody (antibody to HA or TrkB) at 4 °C overnight, followed by incubation with Protein-G–Agarose (Roche) for 2 h at 4 °C. Sedimented complexes were washed four times with immunoprecipitation buffer and resuspended in SDS PAGE loading buffer. Samples were subjected to SDS PAGE and immunoblotted[21].

Lentiviral infection of cortical precursor cells

For lentiviral transduction of DNA constructs into cortical precursor cells, the Lenti-X Lentiviral Expression System from Clontech was used. For the overexpression of fluorescence-tagged dominant-negative c-Src, mutated cDNA from a c-Src (K296R/Y528F)[31] containing expression vector (Millipore) was subcloned into pLV-X-DsRed-Monomer-C1 (Clontech). Dominant-negative Fyn was obtained by subcloning a Fyn (K299M)[32] coding fragment into pLV-X-AcGFP-N1. A GFP control virus was used. Staining for GFP and DsRed was used as a control for equal infection rates of the cell cultures. Cells were pulsed with EGF and processed for western blot or immunofluorescence analysis.

Knockdown of TrkB and TrkC by shRNA in cortical precursor cells

To knock down TrkB and TrkC in cortical precursor cells, we chose[13,52] the target sequences 5′-TTGTGGATTCCGGCTTAAA-3′ for TrkB, 5′-GCAGCAAGACTGAGATCAA-3′ for TrkC1 and 5′-GGACGATGGGAACCTCTTC-3′ for TrkC2 and cloned them into the pSIH-H1 shRNA vector (System Bioscience): shTrkB top-oligo (5′-GATCCTTGTGGATTCCGGCTTAAACTTCCTGTCAGATTTAAGCCGG-AATCCACAATTTTTG-3′), shTrkC1 top-oligo (5′-GATCCGCAGCAAGACT GAGATCAACTTCCTGTCAGATTGATCTCAGTCTTGCTGCTTTTTG-3′), shTrkC2 top-oligo (5′-GATCCGGACGATGGGAACCTCTTCCTTCCTGTC AGAGAAGAGGTTCCCATCGTCCTTTTTG-3′), control top-oligo (5′-gatccT TCTCCGAACGTGTCACGTcttcctgtcagaACGTGACACGTTCGGAGAAttt ttg-3′). Dissociated cortical precursor cells were infected in suspension, plated and harvested after 96 h. Cell lysates were analyzed by western blot analysis.

Analysis of TrkB glycosylation in cortical precursor cells

In vitro deglycosylation of protein lysates from cortical precursor cells was performed with the E-DEGLY enzymatic deglycosylation kit from Sigma, following the instructions of the manufacturer. In brief, 15 μg total protein was subjected to enzymatic digestion with the provided deglycosylating enzymes for 3 h at 37 °C and analyzed by SDS-PAGE and western blotting as described above. Tunicamycin (Sigma) treatment of cortical precursors was performed for 12 h at a concentration of 1 μg ml^{-1}.

Biotinylation of cell-surface proteins

Cells were grown in 100-mm dishes, washed three times with ice-cold HBSS (PAA Laboratories), and incubated for 30 min at 4 °C with 8-ml biotin labeling solution from the surface protein isolation kit from Pierce. After quenching of the biotinylation reaction, cells were washed three times with ice-cold Tris-buffered saline (TBS). EGF treatment was performed for 5 min and PD153035 pre-treatment for 60 min. Cells were harvested in 100 µl immunoprecipitation buffer (25 mM Tris-HCl pH 7.5, 150 mM NaCl, 2 mM EDTA, 2 mM EGTA, 10% glycerol, 0.1% NP-40). Cleared supernatants were applied for protein isolation and elution according to the manufacturer's instruction. Eluted samples were analyzed by standard SDS-PAGE techniques. The densitometric intensity of TrkB-immunoreactive bands was quantified using AIDA software (Raytest). Values were normalized to intensities of pan-cadherin. Values from unstimulated cells not treated with EGF were set as point of reference (100%) in each individual experiment. One sample *t* test was used for statistical analysis.

Immunocytochemistry of cortical precursor cells

Cortical precursor cells maintained as neurosphere cultures were triturated and plated onto 10-mm glass cover slips coated with poly-33-ornithine and Laminin1 at a density of 3,000 cells per cover slip. At given time points, cells were fixed with 4% paraformaldehyde (wt/vol) in 0.15 M phosphate buffer at pH 7.4 for 10 min at 20–25 °C. Cells were rinsed three times with PBS, blocked and permeabilized with blocking buffer (7.5% normal serum (vol/vol), 1% BSA (wt/vol), 0.5% Tween-20 (vol/vol) and 0.05% Triton X-100 (vol/vol) in PBS) for 1 h at 20–25 °C. Primary antibodies were incubated in blocking buffer overnight at 4 °C. Cells were rinsed three times with PBS and incubated with appropriate fluorophor-conjugated secondary antibodies and nuclear dye 4′,6′-diamidine-2′-phenylindole dihydrochloride (DAPI, Sigma, at a final concentration of 5 µg ml^{-1}) for 1 h at 20–25 °C. Cells were washed three times with PBS, mounted on glass slides in MOWIOL and stored at 4 °C.

Immunohistochemistry of frozen tissue sections

For cryosectioning, embryos were fixed overnight in 4% paraformaldehyde (wt/vol) in 0.15 M phosphate buffer at pH 7.4 at 4 °C, and washed three times in PBS followed by dehydration of the tissue in 30% sucrose (wt/vol) overnight at 4 °C. Heads were embedded in OCT Compound (Tissue-Tek) and frozen in liquid nitrogen–cooled 2-methylbutane. We prepared 25-µm coronal frozen sections using a Cryostat (Leica). Glass slides with cryosections were stored at −20 °C. Sections were processed for immunostaining by air drying for 30 min at 20–25 °C and blocking for 1 h at 20–25 °C with 5% normal serum, 0.3% Triton X-100 in TBS. Labeling with primary antibody was performed in blocking buffer overnight at 4 °C in a humidified chamber. Sections were washed three times for 5 min with TBS and incubated with appropriate fluorophor-conjugated secondary antibodies and nuclear dye DAPI (Sigma, at a final concentration of 5 µg ml^{-1}) for 1 h at 20–25 °C. Sections were washed three times with TBS for 5 min and mounted with MOWIOL.

Quantification of *in vivo* incorporated BrdU

Pregnant female mice were intraperitoneally injected with BrdU in sterile 0.9% NaCl (100 mg per g of body weight, Sigma). Embryos were dissected at E16 and processed for 25-μm frozen tissue sections as described above. After incubation with 2 M HCl for 1 h at 20–25 °C, sections were incubated with 0.1 M borate buffer, pH 8.5, washed three times with PBS for 5 min and blocked for 1 h at 20–25 °C with 7.5% donkey serum (vol/vol), 0.3% Triton X-100 in PBS. BrdU antibodies (Abcam ab6326, rat, 1:200 in blocking solution) were incubated overnight at 4 °C followed by secondary Cy3-coupled antibodies (Jackson ImmunoResearch Laboratories #112-165-003, 1:400 in blocking solution) for 1 h at 20–25 °C. Nuclei were stained with DAPI (Sigma, 5 μg ml^{-1}). Sections were washed three times with PBS, mounted with MOWIOL, and BrdU-positive cells were counted in photomicrographic areas of 115 × 115 μm. Every fourth section was subjected to counting, with two location-matched areas per hemisphere (3 animals per genotype, 12 images each). Statistical analysis of total cell numbers was performed using Student's *t* test, and the relative distribution of BrdU-positive cells in layer V versus cortical plate and marginal zone was compared by one-way ANOVA with Bonferroni post testing.

In vitro migration assay

Cortical precursor cell migration was studied with an assay described previously[30,31] with minor changes. 20-mm glass coverslips coated with poly-33-ornithine and Laminin1 received additional substrate carpets consisting of alternating stripes of EGF (100 ng ml^{-1}), BSA (100 ng ml^{-1}) and/or BDNF (20 ng ml^{-1}), with the first set of stripes containing fluorescence-conjugated IgG (2.5 μg ml^{-1}), as outlined in Figure 6. Cortical precursor cells were plated at a density of 2,000 cells per 100 μl. At given time points, cells were fixed, processed for immunocytochemistry, and counted on first and second set of stripes, respectively. A minimum of 150 cells were analyzed per experiment and condition. The results of three independent experiments were pooled.

Quantification of asymmetric pTrk-PLCγ immunoreactivity in stripe assays

Activated TrkB in cortical cells within 30 μm of the EGF stripe in the *in vitro* migration assay was quantified by setting a border in parallel to the EGF stripe through the nucleus so that an area averting from EGF and an area facing EGF could be defined. In both areas, pTrk-PLCγ intensities were measured and compared. A total number of 38 cells from four independent experiments were assessed using Student's *t* test.

Quantitative real-time reverse transcriptase PCR

RNA from cultured cortical precursor cells was isolated by standard protocols using RNeasy Plus-Mini-Kit (Qiagen). Quantitative PCR reactions were run on a Lightcycler 1.5 (Roche) using FastStart DNA master SYBR green1 reagents, using kinetic PCR cycles. Offline analysis to calculate efficiency-controlled relative expression levels was described previously[53]. Intron-spanning primers were selected with Oligo 6.0 software (MedProbe). Reactions were performed in glass capillaries in a volume of 20 μl. Primers and PCR targets: *Ntrk3* (410-for, 5′-TGATCAACAAGTA-TGGTCGC-3′; 1602-rev, 5′-TTGTGACCCTGACGGAAGT-3′; 211 bp). Kinetic cycle conditions in four segments:

Ntrk3 (95 °C, 0 s, 59 °C, 5 s, 72 °C, 9 s, 86 °C, 5 s), 3 mM $MgCl_2$, 30 pmol primer, efficiency = 2.00; *Gapdh* (NM_008084), 205-for 5′-GCAAA-TTCAACGGCACA-3′; 337-rev 5′-CACCAGTAGACTCCACG AC-3′; 141 bp. Kinetic cycle conditions in four segments: *Gapdh* (95 °C, 0 s, 59 °C, 5 s, 72 °C, 6 s, 83 °C, 5 s) 3 mM $MgCl_2$, 30 pmol primer, efficiency: 2.00; *Hmbs*: 252U18-for 5′-AGTGGGCA-CCCGTAAGAG-3′; 350L20-rev 5′-GTCTCCCGTGGTGGACATAG-3′; 118 bp. Kinetic cycle conditions in four segments: *Hmbs* (95 °C, 0 s, 59 °C, 5 s, 72 °C, 6 s, 85 °C, 5 s) 4 mM $MgCl_2$, 30 pmol primer, efficiency: 2.00.

Confocal microscopy

Digital micrographs were acquired with Leica Confocal Software using the Leica SP2 System. Linear contrast and brightness enhancement was similarly applied within corresponding picture groups. Pictures were arranged and labeled with Adobe Photoshop 7.0.

Statistical analysis

Sample size was chosen according to standard practice in the field, taking into account available numbers of cells per *in vitro* experiment or mice from same litters, to allow matched controls in which different genotypes or groups were compared under the same conditions. Densitometric intensities in western blots were normalized to loading controls or total protein levels in case of phospho-specific signals. Values from control conditions in each independent experiment were set as 100%. One-sample *t* test was used to compare the means to this reference value. The intensity of pTrk and phospho-Erk1/2 immunofluorescence signals was measured as arbitrary units per area based on quantum levels per pixel and subjected to statistical analysis, as described previously[54]. Values from at least three independent experiments were pooled, and results were expressed as the mean ± s.e.m. and applied for statistical analysis using GraphPad Prism software. Cells were counted in six sections of a series of coronal 25-μm sections, covering the embryonic telencephalon from rostral to caudal. Forebrains from three mice were used for quantitative analysis of each genotype.

Supplementary Material

Refer to Web version on PubMed Central for supplementary material.

Acknowledgments

We would like to thank M. Sibilia (Medical University of Vienna) for providing $Egfr^{-/-}$ mice, Y.A. Barde (University of Basel) for the HA-TrkB construct, K. Walter for excellent technical assistance, and W. Fouquet and S. Sigrist for their help in STED microscopy. This work was supported by the Deutsche Forschungsgemeinschaft, grants SFB 487, C4 (N.O.) and SFB 581, B4 (D.P. and M.S.), ForNeuroCell (M.S.) and by US National Institutes of Health grant NS21072-24 (M.V.C.).

References

1. Doetsch F, Caille I, Lim DA, Garcia-Verdugo JM, Alvarez-Buylla A. Subventricular zone astrocytes are neural stem cells in the adult mammalian brain. Cell. 1999; 97:703–716. [PubMed: 10380923]

2. Götz M, Huttner WB. The cell biology of neurogenesis. Nat Rev Mol Cell Biol. 2005; 6:777–788. [PubMed: 16314867]
3. Alvarez-Buylla A, Garcia-Verdugo JM, Tramontin AD. A unified hypothesis on the lineage of neural stem cells. Nat Rev Neurosci. 2001; 2:287–293. [PubMed: 11283751]
4. Gupta A, Tsai LH, Wynshaw-Boris A. Life is a journey: a genetic look at neocortical development. Nat Rev Genet. 2002; 3:342–355. [PubMed: 11988760]
5. Angevine JB, Sidman RL. Autoradiographic study of cell migration during histogenesis of cerebral cortex in the mouse. Nature. 1961; 192:766–768. [PubMed: 17533671]
6. Rakic P. Mode of cell migration to the superficial layers of fetal monkey neocortex. J Comp Neurol. 1972; 145:61–83. [PubMed: 4624784]
7. Molyneaux BJ, Arlotta P, Menezes JRL, Macklis JD. Neuronal subtype specification in the cerebral cortex. Nat Rev Neurosci. 2007; 8:427–437. [PubMed: 17514196]
8. Bayer, SA.; Altman, J. Neocortical Development. Raven; New York: 1991.
9. Ayala R, Shu T, Tsai LH. Trekking across the brain: the journey of neuronal migration. Cell. 2007; 128:29–43. [PubMed: 17218253]
10. Rakic P. Evolution of the neocortex: a perspective from developmental biology. Nat Rev Neurosci. 2009; 10:724–735. [PubMed: 19763105]
11. Maisonpierre PC, et al. NT-3, BDNF, and NGF in the developing rat nervous system: parallel as well as reciprocal patterns of expression. Neuron. 1990; 5:501–509. [PubMed: 1688327]
12. Behar TN. Neurotrophins stimulate chemotaxis of embryonic cortical neurons. Eur J Neurosci. 1997; 9:2561–2570. [PubMed: 9517461]
13. Bartkowska K, Paquin A, Gauthier AS, Kaplan DR, Miller FD. Trk signaling regulates neural precursor cell proliferation and differentiation during cortical development. Development. 2007; 134:4369–4380. [PubMed: 18003743]
14. Ernfors P, Lee KF, Jaenisch R. Mice lacking brain-derived neurotrophic factor develop with sensory deficits. Nature. 1994; 368:147–150. [PubMed: 8139657]
15. Ernfors P, Lee KF, Kucera J, Jaenisch R. Lack of neurotrophin-3 leads to deficiencies in the peripheral nervous system and loss of limb proprioceptive afferents. Cell. 1994; 77:503–512. [PubMed: 7514502]
16. Medina DL, et al. TrkB regulates neocortex formation through the Shc/PLCgamma-mediated control of neuronal migration. EMBO J. 2004; 23:3803–3814. [PubMed: 15372074]
17. Lotto RB, Asavaritikrai P, Vali L, Price DJ. Target-derived neurotrophic factors regulate the death of developing forebrain neurons after a change in their trophic requirements. J Neurosci. 2001; 21:3904–3910. [PubMed: 11356878]
18. Xu B, et al. Cortical degeneration in the absence of neurotrophin signaling: dendritic retraction and neuronal loss after removal of the receptor TrkB. Neuron. 2000; 26:233–245. [PubMed: 10798407]
19. Cheng A, Wang S, Cai J, Rao MS, Mattson MP. Nitric oxide acts in a positive feedback loop with BDNF to regulate neural progenitor cell proliferation and differentiation in the mammalian brain. Dev Biol. 2003; 258:319–333. [PubMed: 12798291]
20. Visel A, et al. Regulatory pathway analysis by high-throughput *in situ* hybridization. PLoS Genet. 2007; 3:1867–1883. [PubMed: 17953485]
21. Götz R, et al. Bag1 is essential for differentiation and survival of hematopoietic and neuronal cells. Nat Neurosci. 2005; 8:1169–1178. [PubMed: 16116448]
22. Lee FS, Ragagopal R, Kim AH, Chang P, Chao MV. Activation of Trk neurotrophin receptor signaling by pituitary adenylate cyclase–activating polypeptides. J Biol Chem. 2002; 277:9096–9102. [PubMed: 11784714]
23. Wiese S, et al. Adenosine receptor A2A-R contributes to motoneuron survival by transactivating the tyrosine kinase receptor TrkB. Proc Natl Acad Sci USA. 2007; 104:17210–17215. [PubMed: 17940030]
24. Iwakura Y, Nawa H, Sora I, Chao MV. Dopamine D1 receptor–induced signaling through TrkB receptors in striatal neurons. J Biol Chem. 2008; 283:15799–15806. [PubMed: 18381284]

25. Caric D, et al. EGFRs mediate chemotactic migration in the developing telencephalon. Development. 2001; 128:4203–4216. [PubMed: 11684657]
26. Burrows RC, Wancio D, Levitt P, Lillien L. Response diversity and the timing of progenitor cell maturation are regulated by developmental changes in EGFR expression in the cortex. Neuron. 1997; 19:251–267. [PubMed: 9292717]
27. Sun Y, Goderie SK, Temple S. Asymmetric distribution of EGFR receptor during mitosis generates diverse CNS progenitor cells. Neuron. 2005; 45:873–886. [PubMed: 15797549]
28. Rohrer B, Korenbrot JI, LaVail MM, Reichardt LF, Xu B. Role of neurotrophin receptor TrkB in the maturation of rod photoreceptors and establishment of synaptic transmission to the inner retina. J Neurosci. 1999; 19:8919–8930. [PubMed: 10516311]
29. Rajagopal R, Chao MV. A role for Fyn in Trk receptor transactivation by G protein–coupled receptor signaling. Mol Cell Neurosci. 2006; 33:36–46. [PubMed: 16860569]
30. Lee FS, Chao M. Activation of Trk neurotrophin receptors in the absence of neurotrophins. Proc Natl Acad Sci USA. 2001; 98:3555–3560. [PubMed: 11248116]
31. Mukhopadhyay D, et al. Hypoxic induction of human vascular endothelial growth factor expression through c-Src activation. Nature. 1995; 375:577–581. [PubMed: 7540725]
32. Resh MD. Fyn, a Src family tyrosine kinase. Int J Biochem Cell Biol. 1998; 30:1159–1162. [PubMed: 9839441]
33. Fry DW, et al. A specific inhibitor of the epidermal growth factor receptor tyrosine kinase. Science. 1994; 265:1093–1095. [PubMed: 8066447]
34. Vagin O, Kraut JA, Sachs G. Role of N-glycosylation in trafficking of apical membrane proteins in epithelia. Am J Physiol Renal Physiol. 2009; 296:F459–F469. [PubMed: 18971212]
35. Gut A, et al. Carbohydrate-mediated Golgi to cell surface transport and apical targeting of membrane proteins. EMBO J. 1998; 17:1919–1929. [PubMed: 9524115]
36. Vagin O, Turdikulova S, Sachs G. Recombinant addition of N-glycosylation sites to the basolateral Na,K-ATPase beta1 subunit results in its clustering in caveolae and apical sorting in HGT-1 cells. J Biol Chem. 2005; 280:43159–43167. [PubMed: 16230337]
37. Sibilia M, Wagner EF. Strain-dependent epithelial defects in mice lacking the EGF receptor. Science. 1995; 269:234–238. [PubMed: 7618085]
38. Vielmetter J, Stolze B, Bonhoeffer F, Stuermer CA. *In vitro* assay to test differential substrate affinities of growing axons and migratory cells. Exp Brain Res. 1990; 81:283–287. [PubMed: 2397757]
39. Knöll B, Weinl C, Nordheim A, Bonhoeffer F. Stripe assay to examine axonal guidance and cell migration. Nat Protoc. 2007; 2:1216–1224. [PubMed: 17546017]
40. Paves H, Saarma M. Neurotrophins as *in vitro* growth cone guidance molecules for embryonic sensory neurons. Cell Tissue Res. 1997; 290:285–297. [PubMed: 9321690]
41. Ming GL, et al. Adaptation in the chemotactic guidance of nerve growth cones. Nature. 2002; 417:411–418. [PubMed: 11986620]
42. Dontchev VD, Letourneau P. Nerve growth factor and semaphorin 3A signaling pathways interact in regulating sensory neuronal growth cone motility. J Neurosci. 2002; 22:6659–6669. [PubMed: 12151545]
43. Rajagopal R, Chen ZY, Lee FS, Chao MV. Transactivation of Trk neurotrophin receptors by G protein–coupled receptor ligands occurs on intracellular membranes. J Neurosci. 2004; 24:6650–6658. [PubMed: 15282267]
44. Sibilia M, Steinbach J, Stingl L, Aguzzi A, Wagner EF. A strain-independent postnatal neurodegeneration in mice lacking the EGF receptor. EMBO J. 1998; 17:719–731. [PubMed: 9450997]
45. Doetsch F, Petreanu L, Caille I, Garcia-Verdugo JM, Alvarez-Buylla A. EGF converts transit-amplifying neurogenic precursors in the adult brain into multipotent stem cells. Neuron. 2002; 36:1021–1034. [PubMed: 12495619]
46. Tropepe V, Craig CG, Morshead CM, van der Kooy D. Transforming Growth Factor-alpha Null and Senescent Mice Show Decreased Neural Progenitor Cell Proliferation in the Forebrain Subependyma. J Neurosci. 1997; 17:7850–7859. [PubMed: 9315905]

47. Qiu L, et al. Crosstalk between EGFR and TrkB enhances ovarian cancer cell migration and proliferation. Int J Oncol. 2006; 29:1003–1011. [PubMed: 16964397]

48. Meyer-Franke A, et al. Depolarization and cAMP elevation rapidly recruit TrkB to the plasma membrane of CNS neurons. Neuron. 1998; 21:681–693. [PubMed: 9808456]

49. Li Y, et al. TrkB regulates hippocampal neurogenesis and governs sensitivity to antidepressive treatment. Neuron. 2008; 59:399–412. [PubMed: 18701066]

50. Bergami M, et al. Deletion of TrkB in adult progenitors alters newborn neuron integration into hippocampal circuits and increases anxiety-like behavior. Proc Natl Acad Sci USA. 2008; 105:15570–15575. [PubMed: 18832146]

51. Arévalo JC, et al. Cell survival through Trk neurotrophin receptors is differentially regulated by ubiquitination. Neuron. 2006; 50:549–559. [PubMed: 16701206]

52. Takahashi H, et al. Postsynaptic TrkC and presynaptic PTPsigma function as a bidirectional excitatory synaptic organizing complex. Neuron. 2011; 69:287–303. [PubMed: 21262467]

53. Rasmussen, R. Quantification on the LightCycler. In: Meurer, S., editor. Rapid Cycle Real-Time PCR: Methods and Applications. Springer; Berlin: 2001. p. 21-34.

54. Jablonka S, Beck M, Lechner BD, Mayer C, Sendtner M. Defective Ca^{2+} channel clustering in axon terminals disturbs excitability in motoneurons in spinal muscular atrophy. J Cell Biol. 2007; 179:139–149. [PubMed: 17923533]

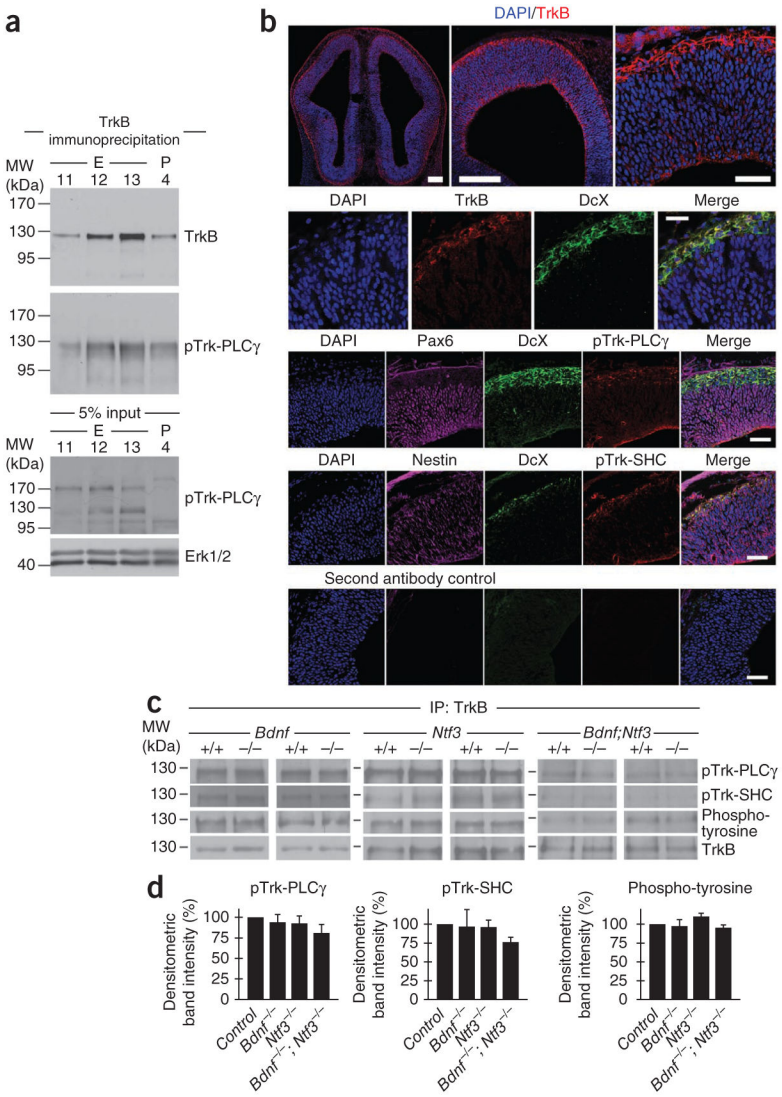

Figure 1.

Expression and activation of TrkB by EGF in cortical precursors. (**a**) TrkB and pTrk-PLCγ levels in embryonic and early postnatal mouse forebrain. (**b**) TrkB and pTrk immunoreactivity in Pax6- and nestin-positive cells of the ventricular zone, and doublecortin (DcX)-positive cells in the early cortical plate. Scale bars represent 150 μm, 50 μm and 25 μm in the top panels (left to right), 25 μm in the middle panels, and 50 μm in the lower panels. (**c**) Levels of TrkB activation after immunoprecipitation of TrkB from E13 forebrain from *Bdnf*$^{-/-}$, *Ntf3*$^{-/-}$ and *Bdnf*$^{-/-}$*; Ntf3*$^{-/-}$ mice, and corresponding wild-type littermates detected with antibodies to pTrk-PLCγ, pTrk-SHC and phospho-tyrosine. (**d**) Quantitative analysis did not reveal significant differences of TrkB activation between *Bdnf*$^{-/-}$, *Ntf3*$^{-/-}$, *Bdnf*$^{-/-}$*; Ntf3*$^{-/-}$ and wild-type mice when tested by one-sample *t* test. Data represent mean ± s.e.m. For full-length blots, see Supplementary Figures 1 and 10.

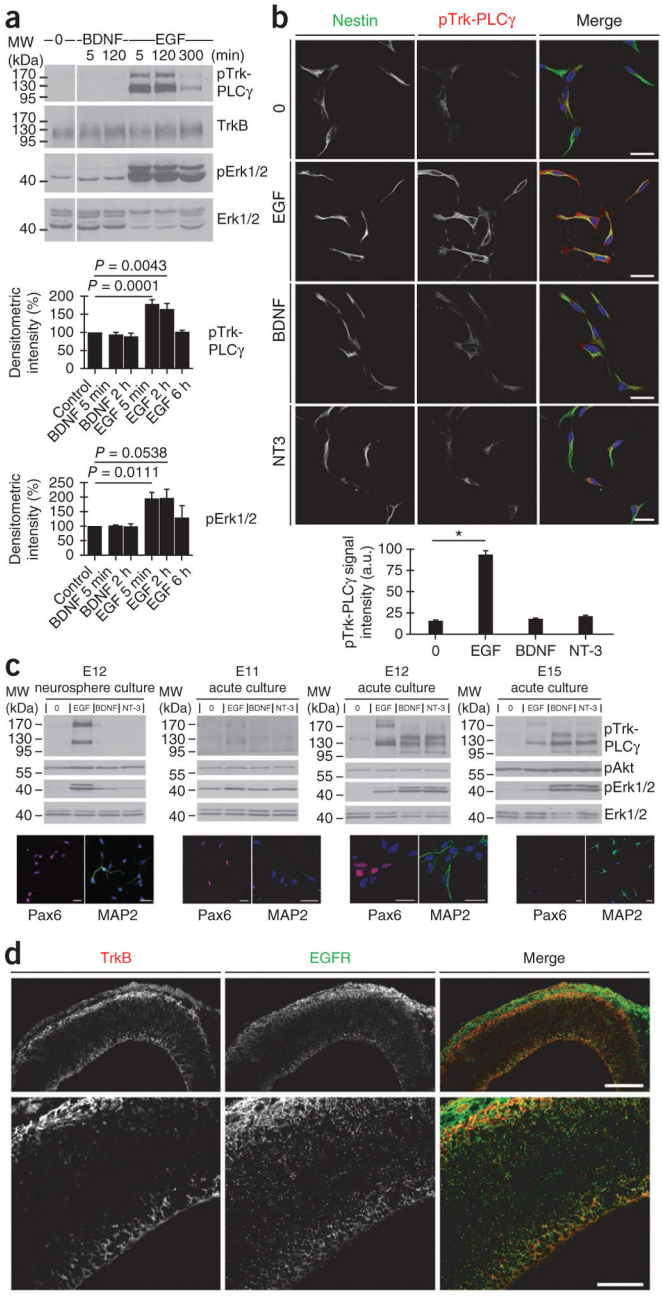

Figure 2.

EGF is the major activator of TrkB in cortical precursor cells. (**a**) EGF, but not BDNF, treatment resulted in phosphorylation of Trk (Trk-PLCγ) and Erk1/2 in cultured forebrain cortical precursor cells. To quantify phosphorylation levels of Trk, we analyzed densitometric scans of immunoblots. Levels of pTrk in unstimulated cells were defined as 100% (mean ± s.e.m., one sample *t* test). (**b**) EGF treatment led to rapid elevation of pTrk-PLCγ immunoreactivity in cultured nestin-positive forebrain cortical precursor cells. Measured intensities are shown as arbitrary units ± s.e.m. (**P* < 0.001, one-way ANOVA). Scale bars represent 25 μm. (**c**) Isolated cortical precursor cells (E12) from neurosphere

cultures consisted mainly of Pax6-positive precursors and showed strong induction of TrkB phosphorylation, but no substantial response to BDNF or NT-3. Similar responses to EGF, BDNF and NT-3 were observed in acutely isolated cortical precursors from E11 forebrain vesicles directly cultured for 24 h. Acutely plated primary cells from E12 forebrain grown for 24 h showed a robust response to EGF, but also to BDNF and NT-3. At E15, the response to BDNF and NT-3 was predominant, although TrkB phosphorylation following EGF treatment was still detectable. From E11 to E15, the percentage of Pax6-positive precursor cells decreased, whereas the percentage of MAP2-positive neurons increased. Scale bars represent 25 μm. (**d**) Coexpression of EGFR and TrkB in E13 forebrain. Scale bars represent 150 μm (top panels) and 50 μm (lower panels). For full-length blots, see Supplementary Figure 10.

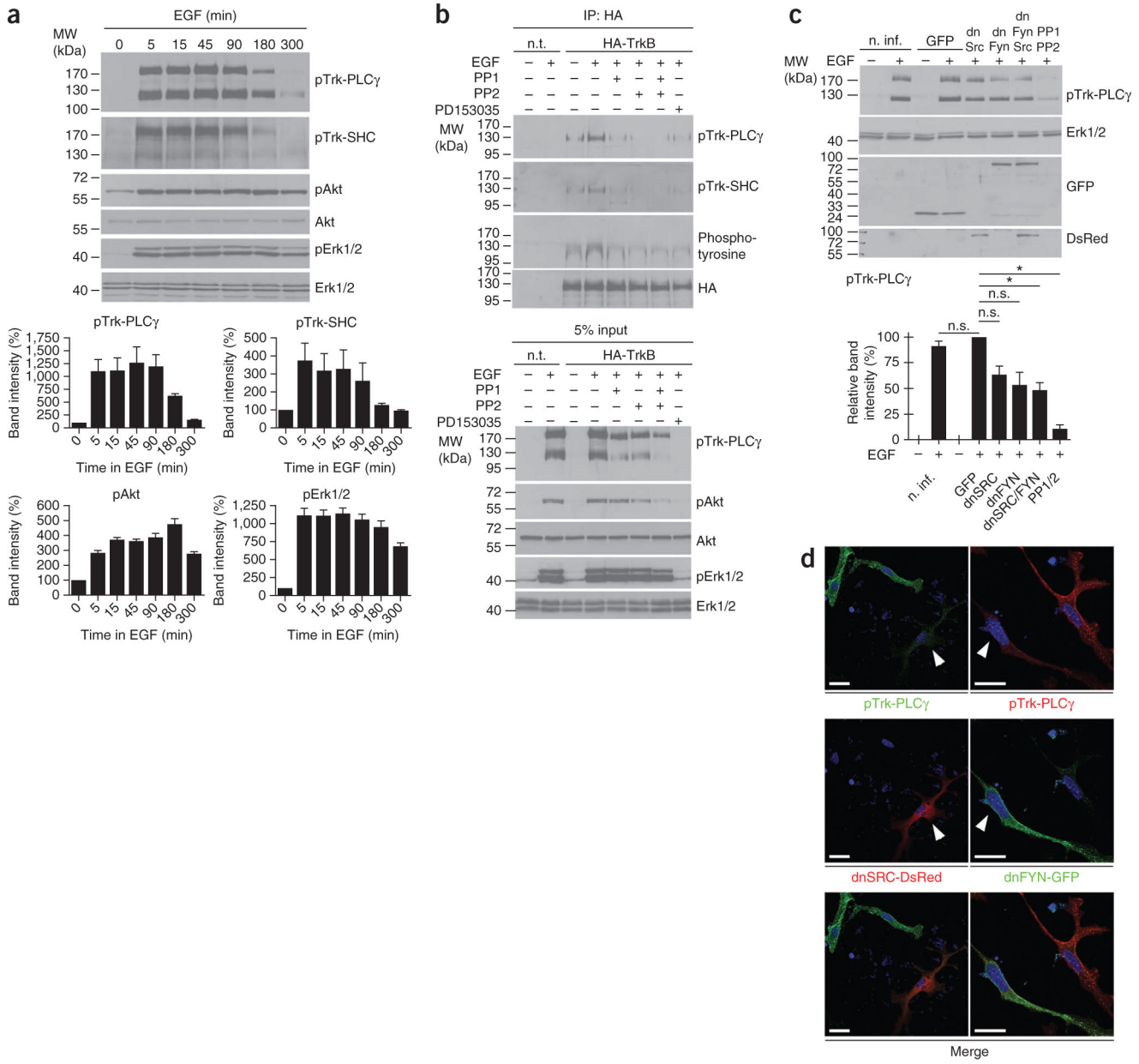

Figure 3.

Characterization of TrkB transactivation by EGFR signaling. (**a**) Phosphorylation of Trk receptors by EGF treatment at both the PLCγ- and SHC-binding domains. Activation correlated with phosphorylation of Akt (Ser473) and Erk1/2. Time-dependent phosphorylation of Trk, Erk1/2 and Akt was quantified by measuring intensities of densitometric immunoblot scans from three independent experiments. After normalization with loading controls, values of untreated cells were set to 100%. Data represent mean ± s.e.m. (**b**) Transactivation of TrkB by EGFR signaling was blocked by Src family kinase inhibitors PP1 (1 μM) and PP2 (100 nM) and the EGFR inhibitor PD153035 (100 nM). (**c**) Western blot analysis of cell cultures treated with a GFP control lentivirus, dnSRC, dnFYN lentivirus or a combination of dnSRC and dnFYN. Trk-PLCγ immunoreactive bands were

significantly reduced in dnSRC- and dnFYN-treated cells. The lower panel shows quantitative analyses of densitometric immunoblot scans from three independent experiments (*$P < 0.05$, mean ± s.e.m., one sample *t* test). (**d**) dnSRC-DsRed was overexpressed as a fusion protein using a lentivirus. Positively infected cells, in comparison with uninfected cells in the same cultures, showed reduced pTrk-PLCγ immunoreactivity after EGF treatment. Similar observations were made with cells infected with a lentivirus encoding a dnFYN-GFP fusion protein. Arrowheads point to positively infected cells. Scale bars represents 10 μm. For full-length blots, see Supplementary Figure 10. n.t., not transfected; n. inf, not infected; n.s., not significant ($P > 0.05$).

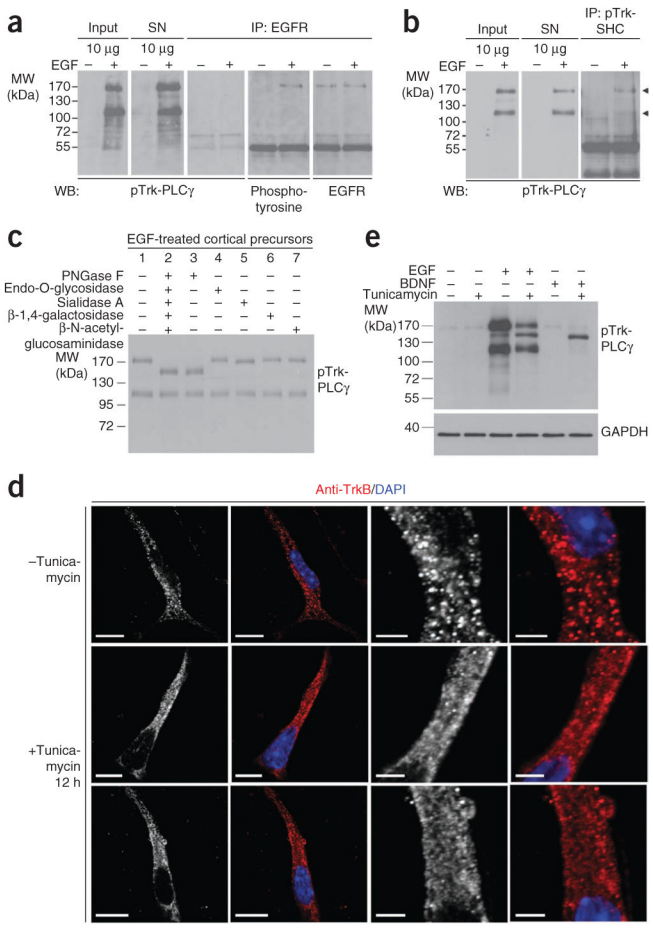

Figure 4.

Characterization of the 170-kDa band recognized by the pTrk-PLCγ antibody. (**a**) After immunoprecipitation of EGFR, no signal was detectable in the precipitate when probed with antibody to pTrk-PLCγ (third panel from the left), indicating no crossreactivity of antibody to pTrk-PLCγ with EGFR. Positive controls with antibodies to phospho-tyrosine and EGFR revealed that EGFR was present in the precipitate and activated following stimulation with EGF. (**b**) After immunoprecipitation with antibody to pTrk-SHC, both bands at 170 kDa and 130 kDa were detectable in the precipitate when probed with antibody to pTrk-PLCγ (third panel from the left). (**c**) Deglycosylation of EGF-treated cortical precursor cells with PNGase F shifted the 170-kDa Trk-immunoreactive band to about 145 kDa. Other deglycosylating enzymes that cleave processed glycosyl side chains typically found in cell surface proteins were not effective. The relative specificity of PNGase F indicated that Trk receptors are heavily N-glycosylated in early cortical neural precursor cells. (**d**) Immunostaining revealed that TrkB was localized intracellularly in untreated cortical precursor cells. After treatment with tunicamycin, which specifically inhibits the transfer of N-actelyglucosamine-1-phosphate in the first step of N-glycosylation, TrkB became detectable at the cell membrane. Scale bars represent 10 µm (left) and 3 µm (right). (**e**) Treatment of cortical precursor cells with tunicamycin for 12 h shifted the 170-kDa band for

N-glycosylated Trk to 130 kDa. This treatment also restored BDNF responsiveness, indicating that tunicamycin reversed the retention of TrkB in an intracellular compartment.

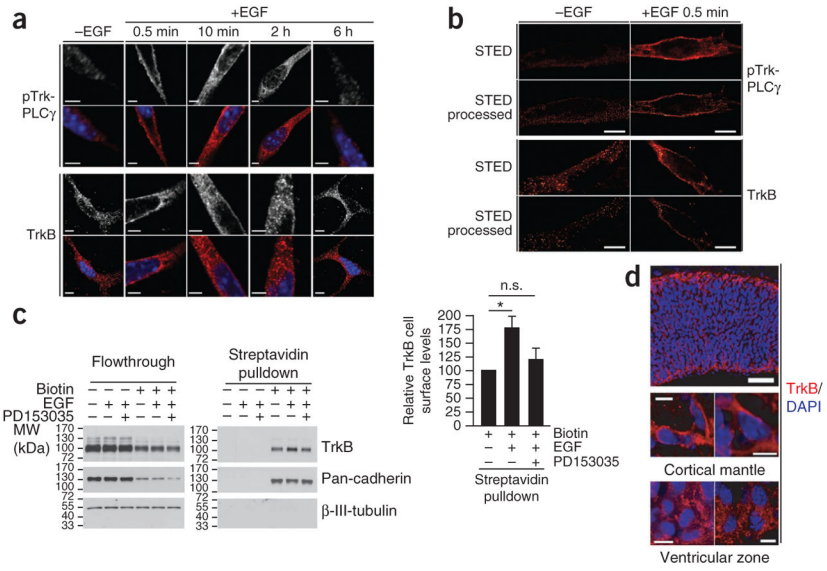

Figure 5.

Translocation of TrkB to the cell surface of cortical precursor cells in response to EGF. (**a**) TrkB immunoreactivity was localized predominantly in dot-like intracellular structures of cultured E12 neurosphere-derived cortical precursor cells and translocated to the membrane within 0.5 min of EGF treatment. Scale bars, 3 μm. (**b**) High-resolution STED microscopy identified TrkB in vesicle-like structures in untreated cultured E12 neural precursor cells. Following EGF challenge, signals for TrkB and pTrk-PLCγ showed a rapid translocation to a cell surface–like localization. Scale bars, 3 μm. (**c**) Avidin pulldown after biotinylation of cell surface proteins identified rapid cell surface translocation of TrkB after EGF treatment. The amount of cell surface TrkB that could be pulled down was reduced by simultaneous blockade of EGFR with 100 nM PD153035 (*$P < 0.05$, mean ± s.d. from three independent experiments, one-sample *t* test; n.s., not significant). (**d**) TrkB was mainly detectable in punctate vesicle-like structures in neural precursor cells of the ventricular zone and SVZ, whereas its localization changed to a more cell surface–like distribution in neurons in the cortical mantle zone. Scale bars, 50 μm (top panel) and 3 μm (lower panels). Full-length blots in Supplementary Figure 10.

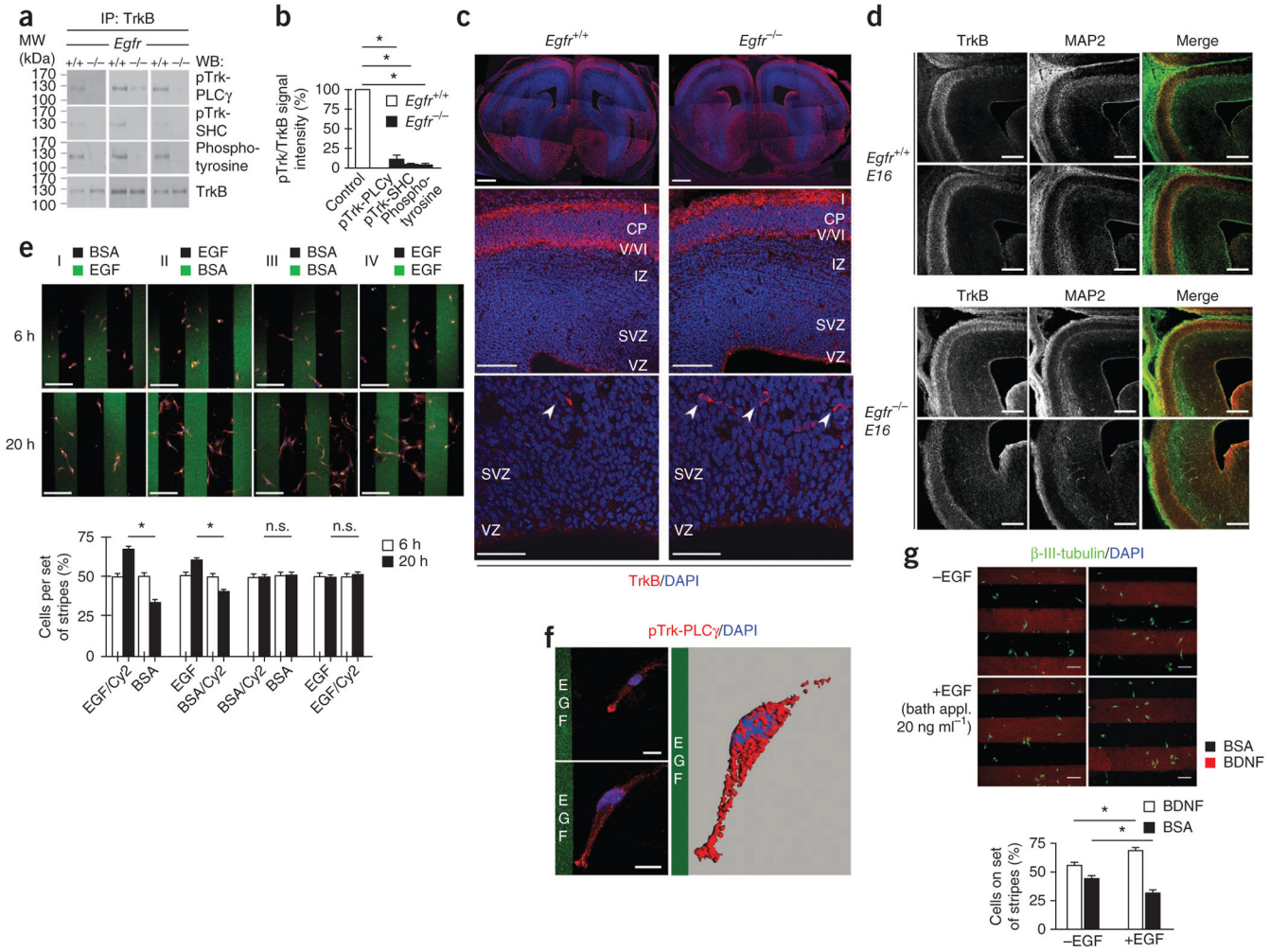

Figure 6.

Reduced transactivation of TrkB in *Egfr*$^{-/-}$ mice affects the formation of the cortical plate. (**a**) Reduced TrkB phosphorylation in *Egfr*$^{-/-}$ forebrain at E13. (**b**) Quantitative analysis of immunoblot signals for pTrk-PLCγ, pTrk-SHC and phospho-tyrosine in wild-type and *Egfr*$^{-/-}$ forebrain (*$P < 0.005$, $n = 3$, mean ± s.e.m., one sample *t* test). (**c**) At E16, the number of neurons in deeper layers of the cortical plate later forming layer V/VI was reduced, whereas the number of TrkB-positive cells in the marginal zone, cortical plate (CP) and SVZ was increased. Scale bars represent 150 μm (top), 100 μm (middle) and 50 μm (bottom). IZ, intermediate zone; VZ, ventricular zone. (**d**) The TrkB-positive cell population that is increased in the SVZ of E16 *Egfr*$^{-/-}$ forebrain coexpressed the neuronal marker MAP2. Scale bars represent 150 μm. (**e**) Stripe assays with EGF and BSA bound to different areas of a culture dish. Quantitative analysis of TrkB- and nestin-positive cells 20 h after plating revealed a significant increase of cells on EGF-coated stripes in comparison with BSA-coated stripes (*$P < 0.001$, mean ± s.e.m., one-way ANOVA; n.s., not significant). Scale bars, 100 μm. (**f**) Individual precursor cells at 6 h after seeding onto a BSA- and EGF-coated stripe substrate. pTrk-PLCγ staining accumulated at the migration front toward the EGF substrate. Scale bars, 10 μm. (**g**) Migration of cortical cells toward BDNF was

enhanced in the presence of EGF. Scale bars, 50 μm. Data are presented as mean ± s.e.m. *P < 0.001. For full-length blots, see Supplementary Figure 10.